Science of the Total Environment 721 (2020) 137663

Contents lists available at ScienceDirect

Science of the Total Environment

journal homepage: www.elsevier.com/locate/scitotenv

Effects of mineral substrate on ectomycorrhizal fungal colonization and bacterial community structure

Qibiao Sun [a,b,1], Xiuming Liu [c,d,1], Shijie Wang [c,d,**], Bin Lian [b,*]

[a] College of Pharmacy and Life Sciences, Jiujiang University, Jiujiang 332000, China
[b] College of Marine Science and Engineering, College of Life Sciences, Nanjing Normal University, Nanjing 210023, China
[c] State Key Laboratory of Environmental Geochemistry, Institute of Geochemistry, Chinese Academy of Sciences, Guiyang 550002, China
[d] Puding Karst Ecosystem Research Station, Chinese Ecosystem Research Network, Chinese Academy of Sciences, Puding 562100, China

HIGHLIGHTS

- Different mineral-fill mesh bags were colonized by different ECM fungi.
- ECM fungi affect bacterial diversity based on mineral types.
- Signal transduction of bacteria was more active in mineral-filled mesh bags.

GRAPHICAL ABSTRACT

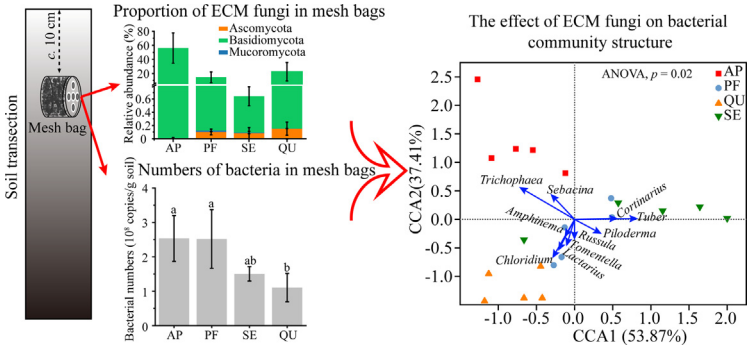

ARTICLE INFO

Article history:
Received 6 December 2019
Received in revised form 29 February 2020
Accepted 29 February 2020
Available online 2 March 2020

Editor: Charlotte Poschenrieder

Keywords:
Ectomycorrhizal fungi
Mesh bags
Trichophaea
Bioweathering
High-throughput sequencing
Bacterial diversity

ABSTRACT

Ectomycorrhizal (ECM) fungi can promote the nutrient uptake of plants from soil minerals by bioweathering. However, effects of different minerals on ECM fungal colonization and bacterial community structures in the soil remains poorly documented. Here, we investigated ECM fungal composition and bacterial communities in different mineral-filled mesh bags buried in forest soil. Control (filled with quartz, which has little nutrients for plants) and mineral (apatite, potash feldspar and serpentine) -filled mesh bags were buried in E-horizon soil for six months. After incubation, the contents of available elements in bags were determined, bacterial population sizes were quantified by quantitative PCR, and bacterial and ECM fungal community structures in mesh bags were assessed using high-throughput sequencing. The results showed that dozens of ECM fungal species colonized in different mesh bags, of which 17, 54 and 47 ECM species were observed in apatite-, potash feldspar- and serpentine-filled bags, respectively. Ectomycorrhizal fungal composition and bacterial community structure are affected significantly by mineral types. *Pseudomonas*, *Sphingomonas*, *Bacillus* and *Paenibacillus*, known for high weathering potential, were the preponderant bacteria in mineral-filled bags compared to the control. Ectomycorrhizal fungi are able to selectively colonize mesh bags based on mineral types, and may have a certain influence on the formation of bacterial community structure, implying a possible cooperation of ECM fungi and bacteria in soil mineral weathering.

* Correspondence to: B. Lian, Nanjing Normal University, Nanjing 210023, China.
** Correspondence to: S. Wang, Institute of Geochemistry, Chinese Academy of Sciences, Guiyang 550002, China.
E-mail addresses: wangshijie@vip.skleg.cn (S. Wang), bin2368@vip.163.com (B. Lian).
[1] Qibiao Sun and Xiuming Liu have contributed equally to this work.

https://doi.org/10.1016/j.scitotenv.2020.137663
0048-9697/

1. Introduction

Ectomycorrhizal (ECM) fungi can improve the uptake of mineral nutrients from soils of trees, such as nitrogen (N), phosphorus (P) and kalium (K); in return, the fungi obtain photosynthetically-fixed carbon from their tree hosts (Landeweert et al., 2001; Smith and Read, 2008). Many studies revealed that ECM fungi are able to promote the uptake of mineral nutrients of plants through weathering soil minerals (Wallander, 2000; Blum et al., 2002; Bonneville et al., 2009; Bonneville et al., 2016). Smits et al. (2012) quantified apatite weathering by the ECM fungus *Paxillus involutus* growing in symbiosis with *Pinus sylvestris* in monoxenic (only contain *P. involutus* without other microorganisms) microcosms, showing that fungal colonization increases the release of P from apatite and improves the biomass and P content of the plant host. Although many ECM fungi such as *Paxillus*, *Pisolithus*, *Rhizopogon*, *Suillus*, etc. can acquire nutrients from minerals (Paris et al., 1996; Wallander, 2000; Wallander et al., 2002; Bonneville et al., 2009), the weathering ability of different ECM species or strains is still greatly different (Lapeyrie et al., 1991; van Schöll et al., 2006). To date, large gaps remain in our understanding of ECM fungi with distinct weathering abilities to obtain nutrients from minerals to supply their tree hosts.

The study of Uroz et al. (2007) revealed that the frequency and weathering efficacy of mineral-weathering bacteria in *Scleroderma citrinum* ectomycorrhizosphere (the volume of soil under the influence of ECM roots, normally around 2–3 mm in scale) is greater than those in the corresponding bulk soil, and raised the hypothesis that by fungal carbon metabolism ECM fungi select a bacterial community with high weathering potential from bulk soil pool. Based on cultivation-dependent method, Calvaruso et al. (2010) showed a significant enrichment of bacterial isolates with efficient mineral weathering potentials around the *Scleroderma citrinum*-oak (*Quercus sessiliflora*) mycorrhizosphere compared to the bulk soil. The enrichment of mineral-weathering bacteria to promote mineral weathering may be an important way of some ECM fungi to compensate for their own limited ability in mineral weathering (Sun et al., 2019). There are many different types of mineral-weathering bacteria in the soil (for a review, see Uroz et al., 2009), of which *Burkholderia*, *Collimonas*, *Pseudomonas* and *Sphingomonas* are common mineral-weathering bacteria in ectomycorrhizosphere. Ectomycorrhizal fungi are capable of selecting specific *Pseudomonas fluorescens* populations that can dissolve inorganic phosphates and chelate iron ions by producing higher levels of siderophores (small, high-affinity iron chelating compounds secreted) to promote plant nutrition indirectly (Frey-Klett et al., 2005). However, it is still poorly understood that whether different ECM fungal species can choose different mineral-weathering bacteria to efficiently obtain nutrients in minerals.

Wallander et al. (2001) developed an in-growth mesh bag method, which is greatly beneficial to study ECM fungi in soils. Mesh bags are filled with sand and buried in the soil, allowing the in-growth of fungal hyphae but excluding fine roots. Ectomycorrhizal fungi, symbiotically associated with plants, can obtain carbohydrates continuously from plant host and possess efficient underground mycelial transport network, so they are able to colonize the environments without or with low organic matter. In contrast, the dispersal of saprotrophic fungi highly depends on the organic matter in the soil and they cannot colonize large areas with low-organic substrates (Ekblad et al., 2016). The in-growth mesh bag method has been extensively applied to study the mycelial growth and nutrient acquisition of mycorrhizal fungi in field (Koele et al., 2014; Averill and Hawkes, 2016; Hagenbo et al., 2017).

In the present study, the aim was to reveal the effects of mineral types for ECM fungal and bacterial colonization. The mineral-filled mesh bags were buried in forest soil for six months. The composition of ECM species and bacterial community structure in the control and mineral-filled bags were analyzed using high-throughput sequencing. Bacterial population sizes in mesh bags were determined by quantitative PCR (qPCR) as well. We hypothesized that a) ECM fungi have a preference for mineral types in colonization and, b) along with minerals, have an impact on bacterial communities.

2. Materials and methods

2.1. Mineral information

The analytical quality pure quartz (≥99.0%, 200–450 μm) used in this study was purchased from Tianjin Kemiou Chemical Reagent Co., Ltd, China. Apatite was from Kaiyang Country, Guizhou Province, China, mainly composed of fluorapatite (45.6%) and hydroxyapatite (41.2%). The elemental composition of the apatite tested by X-ray fluorescence (XRF) was as follows: O 77.35%, Ca 11.10%, P 6.09%, F 1.58%, Mg 1.36%, Si 1.33%, Al 0.35%, Fe 0.29%, Sr 0.23%, K 0.19%, S 0.06%, I 0.06% and Y 0.01%. Potash feldspar was from Fengxian Country, Jiangsu Province, China, mainly composited of muscovite (38.5%), orthoclase (35.2%), quartz (16.3%), and clinochlore (5.3%) according to the data of Wang et al. (2018). The element composition of the potash feldspar tested by XRF was as follows: O 86.57%, Si 6.69%, Al 2.57%, K 1.65%, Fe 1.15%, Mg 0.75%, Ca 0.31%, S 0.12%, Ti 0.10% Na 0.07% and Rb 0.01%. Serpentine was from Donghai Country, Jiangsu Province, China, mainly composed of chrysotile (55.4%) and Fe-containing olivine (24.4%). The elemental composition of the serpentine tested by XRF was as follows: O 46.39%, Mg 23.35%, Si 20.34%, Fe 5.30%, C 3.46%, Al 0.39%, Ni 0.24%, Cr 0.21%, Ca 0.16%, Mn 0.09%, S 0.04%, K 0.02% and Co 0.02%. The mineral samples of feldspar, serpentine and apatite were ground, sieved to collect the 75–150 μm fraction. All mineral samples were cleaned using the method of Sun and Lian (2019).

2.2. Mesh bags setting and cultivation

The mesh bag was modified from Heinemeyer et al. (2007), which was constructed of a polyethylene bottle (6 cm high × 8 cm diameter) filled with mineral powders by covering nylon mesh (48 μm) and a lid (containing five pores, diameter = 1.2 cm), a schematic treatment design is shown in Fig. S1a. In this study, four treatments were set: the apatite-filled bags (AP), 50 g apatite + 250 g quartz; the potash feldspar-filled bags (PF), 50 g potash feldspar + 250 g quartz; the serpentine-filled bags (SE), 50 g serpentine + 250 g quartz; the control bags (QU), 300 g quartz. Each treatment was carried out in quintuplicate.

The experiment site was situated within a mixed forest of Xianlin Campus of Nanjing Normal University in Nanjing, China (32°06′55″ N, 118°54′46″ E), mainly dominated by *Pinus massoniana*, *Quercus serrata*, *Quercus fabri* and *Liquidambar formosana*. The soil pH_{H2O} (pH measured using deionized water) in the forest is 6.80. The available contents of K, P and Mg in forest soil are 77.17 mg/kg soil, 0.21 mg/kg soil and 122.68 mg/kg soil, respectively. Control and mineral-filled mesh bags were buried in groups in E-horizon soil, where the fungi have been shown to be mainly of ECM origin (Wallander et al., 2001; Genney et al., 2006; Lindahl et al., 2007). Each group contains four different mesh bags. As shown in Fig. S1, the mesh bag groups were buried in a 5 m × 5 m quadrat in the forest for about six months (183 days), and were removed for analysis after incubation. Each sample was divided into two subsamples. One of subsamples was air-dried for physico-chemical analysis and the other subsample was stored at −80 °C until the extraction of total DNA.

2.3. Physicochemical assays of substrate in mesh bags

Soil pH_{H2O} was determined at a 1:2.5 (w/v) soil-to-solution ratio with CO_2-free deionized water. The available elements in mesh bags were extracted using AB-DTPA multi-extractant (Soltanpour, 1985) and determined using an inductively coupled plasma emission spectrometer IRIS Intrepid II XSP (Thermo Electron, USA).

2.4. High-throughput sequencing

Microbial DNA was extracted from mineral powders in mesh bags using the FastDNA® Spin Kit for Soil (MP Biomedicals, USA) according to manufacturer's protocols. The final DNA concentration and purity were determined by NanoDrop 2000 UV–vis spectrophotometer (Thermo Scientific, USA), and DNA quality was checked by 1% agarose gel electrophoresis. The V3–V4 hypervariable regions of bacteria 16S rRNA gene were amplified with primers 338F (5′-ACTCCTACGGGAGG CAGCAG-3′) and 806R (5′-GGACTACHVGGGTWTCTAAT-3′) using a Thermocycler GeneAmp 9700 (Applied Biosystems, USA). The ITS1 region of fungi was amplified with ITS1_F (5′-CTTGGTCATTTAGAGGAAG TAA-3′) (Gardes and Bruns, 1993) and ITS2 (5′-GCTGCGTTCTTCATCG ATGC-3′) (White et al., 1990). The PCR reactions were conducted using the following program: 5 min of denaturation at 95 °C, 15 cycles of 1 min at 95 °C, 1 min for annealing at 50 °C, and 1 min for elongation at 72 °C, and a final extension at 72 °C for 7 min. PCR reactions were performed in triplicate 50 μL mixture containing 10 μL of 5 × Q5@ Reaction Buffer, 10 μL of 5 × Q5@ High GC Enhancer, 1.5 μL of 2.5 mM dNTPs, 1.5 μL of each primer (10 μM), 0.2 μL of Q5@ High-Fidelity DNA Polymerase (New England Biolabs, USA) and 50 ng of template DNA. The resulted PCR products were extracted from a 2% agarose gel and further purified using the AxyPrep DNA Gel Extraction Kit (Axygen Biosciences, USA) and quantified using QuantiFluor™-ST (Promega, USA) according to the manufacturer's protocol. Library construction used universal Illumina adaptors and index sequences. Amplicon sequencing was performed on the Illumina HiSeq 2500 platform at Biomarker Technologies Co., Ltd, Beijing, China (http://www.biomarker.com.cn).

Raw paired-end reads of bacterial 16S rRNA V3-V4 regions were demultiplexed, quality-filtered using Trimmomatic version 0.36 with the following criteria: 1) The reads were truncated at any site receiving an average quality score <20 over a 50 bp sliding window; 2) primers were exactly matched allowing two nucleotide mismatching, and reads containing ambiguous bases were removed. Then, the quality-filtered reads were merged using FLASH version 1.2.11 (Magoč and Salzberg, 2011) and chimeric sequences were picked out and removed using the UCHIME algorithm (Edgar et al., 2011) in USEARCH version 8.1 (Edgar, 2013). The processed sequences were clustered into operational taxonomic units (OTUs) at 97% similarity using the UPARSE algorithm in USEARCH. A representative sequence with the highest abundance in each OTU was selected for taxonomic assignment. Taxonomic annotation of representative sequences was performed by RDP Classifier version 2.2 (http://rdp.cme.msu.edu) against the Silva 16S rRNA database using a confidence threshold of 80%. For the ITS1 data, we processed them as for the 16S rRNA gene data and using the UNITE database version 7.2 (Kõljalg et al., 2013). Finally, to ensure a fair comparison between samples, all samples were normalized to the minimum number of sequences. Subsequent analyses were based on the normalized data. The ITS1 OTUs belonging to the ECM fungal taxa were picked out according to list summarized by Tedersoo et al. (2010).

The PICRUSt (phylogenetic investigation of communities by reconstruction of unobserved states) analysis was carried out to predict the functional traits of microbial communities using the 16S rRNA gene sequences employing the KEGG database (Langille et al., 2013). Then, the results were exported for later analysis in a table format using STAMP v2.1.3 (Parks et al., 2014). The raw sequencing data of bacterial 16S rRNA V3–V4 regions and fungal ITS1 region were deposited in the NCBI Sequence Read Archive (SRA) database under the BioProject PRJNA495753.

2.5. Quantification of bacterial population sizes in mesh bags

The qPCR of bacterial 16S rRNA gene was performed in triplicate on an ABI StepOne™ Real-Time PCR system (Applied Biosystems, USA) using primer sets 338F/518R (5′-ATTACCGCGGCTGCTGG-3′). Each 20 μL of qPCR reaction contained 10 μL of AceQ® SYBR Green Master mix (Vazyme Biotech Co., Ltd, China), 0.4 μL of each primer (10 μM), and 1 μL of diluted DNA template and adjusted with RNase-free ddH_2O to the final volume. Amplification of the 16S rRNA gene was conducted using an initial denaturation step at 95 °C for 5 min, followed by 40 cycles of 10 s at 95 °C, 30 s at 60 °C. Melting curve analysis was carried out to verify amplicon specificity. A negative control without DNA template was employed in all of the qPCR amplifications. Standard curve was generated based on decimally diluted standard 16S rRNA gene from *Escherichia coli* DH5α cloned into *pEASY*®-Blunt Zero vector (TransGen Biotech Co., Ltd, China).

2.6. Statistical analyses

The α-diversity indices (Shannon, Simpson, Chao1) of bacterial community in all samples were analyzed in Mothur version 1.30 (Schloss et al., 2009) using default parameters. Non-metric multidimensional scaling (NMDS) analysis, canonical correspondence analysis (CCA), ADONIS (permutational MANOVA) with 999 permutations and mantel test were performed using the *Vegan* package in R version 3.4.3 (R Core Team, 2016). *t*-Test and one-way ANOVA followed by Tukey's HSD tests at $p < 0.05$ were performed in SPSS 20.0. The data represent the mean ± SD (standard deviation) for five independent replicates.

3. Results

3.1. Substrate characteristics in mesh bags

After a 6-month incubation, the contents of available elements in the in-growth mesh bags were determined (Table 1). In the AP treatment, the contents of available Ca and P were higher than other mesh bags ($p < 0.05$). In the PF treatment, the contents of available Ca and Mg were higher than those in both SE and QU treatments. The contents of available Fe and K were the highest compared to other treatments ($p < 0.05$). In the SE treatment, the content of available Mg was the highest ($p < 0.05$). However, the content of available Si was the highest in the QU treatment. The pH_{H2O} value in mesh bags was also altered (Fig. 1). The pH_{H2O} values in AP and SE treatments were increased significantly ($t = 5.743$, $p < 0.05$; $t = 18.839$, $p < 0.05$), which may be due to the consumption of acid matter during weathering and the releasing of basic metals from minerals. However, the pH_{H2O} values in PF and QU treatments had no significant changes ($t = 2.120$, $p > 0.05$; $t = 0.704$, $p > 0.05$).

3.2. Community composition of ECM fungi in mesh bags

Through sequencing of the fungal ITS1 region, a total of 1,844,310 fungal sequences were obtained. 548 fungal genera were detected in the mesh bags, of which 33 genera were ECM. Fig. 2 shows the proportion of ECM sequences in different mesh bags. The proportion of ECM sequences in the AP treatment was 55.92 ± 21.04%. The proportion of ECM sequences in the PF treatment was 14.91 ± 7.86%, lower than the control mesh bags (22.62 ± 12.93%). In the SE treatment, the proportion of ECM fungi was the lowest, only accounting for 0.68 ± 0.20%. The detected ECM genera belonged to three phyla, which are Ascomycota, Basidiomycota and Mucoromycota.

The species and relative abundance of ECM fungi observed in different treatments were notably distinct (Table S1). In the AP treatment, 17 ECM OTUs were found belonging to 12 genera. In the PF treatment, 54 ECM OTUs were found belonging to 27 genera, of which *Clavariadelphus*, *Geopora* and *Sistotrema* were exclusive in this treatment. In the SE treatment, 47 ECM OTUs were found belonging to 23 genera, of which *Gyroporus*, *Scleroderma* and *Pseudotomentella* were exclusive compared to other treatments. In the QU treatment (the control), 38 ECM OTUs were found belonging to 22 genera. *Ceratobasidium*, *Chloridium*, *Cortinarius*, *Lactarius*, *Piloderma*, *Russula*, *Sebacina*, *Trichophaea* and

Table 1
Concentration of available elements in mesh bags of different treatments.

Treatment	Ca	Fe	K	Mg	Mn	P	Si
	mg/kg soil						
AP	1120.84 ± 61.88a	129.24 ± 37.72b	10.84 ± 3.66b	42.57 ± 8.87c	9.53 ± 0.87c	133.72 ± 12.37a	5.55 ± 1.39b
PF	692.37 ± 18.07b	603.96 ± 30.51a	55.39 ± 2.35a	294.56 ± 6.31b	18.15 ± 1.43b	1.53 ± 1.53b	3.57 ± 2.76b
SE	99.15 ± 2.95c	580.97 ± 16.73a	3.59 ± 1.38c	1619.39 ± 74.22a	25.67 ± 1.89a	ND	5.92 ± 2.77b
QU	87.13 ± 5.28c	3.33 ± 0.28c	1.47 ± 0.78c	7.74 ± 2.14c	ND	0.69 ± 0.19b	15.79 ± 8.42a

Different letters indicate significant differences of elemental concentration among different treatments based on Tukey's HSD tests at $p < 0.05$. AP: apatite-filled mesh bags, PF: potash feldspar-filled mesh bags, QU: the control mesh bags, SE: serpentine-filled mesh bags. ND: not detected.

Tuber were shared in the mineral-filled mesh bags and the control. *Trichophaea*, an ECM genus confirmed by Tedersoo et al. (2006), is the most dominant in different treatments.

3.3. Bacterial diversity and functional traits in mesh bags

A total of 1,386,109 clean sequences were obtained from 1,524,457 raw sequences of bacterial V3-V4 regions and 6945 OTUs were obtained after clustering. The amount of observed OTUs in the QU treatment was significantly higher than those in the PF and SE treatments (Table 2). Both of the number of observed OTU and predicted OTU (Chao1 index) did not revealed significant differences between the AP and QU treatments. The amount of OTUs in the SE treatment was the lowest in all treatments. The diversity indices (Chao1, Shannon and Simpson) in the SE treatment were significantly lower than other treatments. In addition, the data of Shannon and Simpson indices showed that the QU treatment possessed the highest bacterial diversity.

Fig. 3 shows the bacterial composition at phylum and class levels in all mesh bags. Acidobacteria, Actinobacteria, Bacteriodetes, Chloroflexi, Firmicutes, Gemmatimonadetes, Nitrospirae, Planctomycetes, Proteobacteria and Verrucomicrobia were the dominant bacteria in the mesh bags, accounting for 87.66–96.48% of the bacterial sequences. In the PF treatment, the relative abundance of Proteobacteria was higher than that in other treatments (71.19 ± 3.30%). In the SE treatment, the relative abundance of Firmicutes was the highest, while the proportions of Acidobacteria (2.72 ± 0.87%) and Chloroflexi (0.54 ± 0.28%) were notably lower than those in other treatments. In the QU treatment (the control), the abundance of Actinobacteria (10.02 ± 1.23%) was higher than that in the AP (4.82 ± 1.90%), PF (5.01 ± 0.88%) and SE (4.44 ± 0.12%) treatments. The differentiation of the bacterial communities in mesh bags was also observed at the class level (Fig. 3b). α-Proteobacteria (37.78 ± 5.38%) and Bacilli (19.21 ± 8.34%) were dominant in the SE treatment compared to other treatments. However, the relative abundance of β-Proteobacteria and γ-Proteobacteria in the PF treatment was the highest, accounting for 20.76 ± 3.81% and 27.38 ± 1.49%, respectively.

At the level of genus, the composition of bacterial community structure in different mesh bags was different as well. The relative abundance of top 50 genera among treatments was significantly different (Fig. 4). The results of NMDS analysis showed that the bacterial community structure in different treatments was significantly distinct (Fig. 5a). It was worth noting that the bacterial community structure in the SE treatment was much different from other treatments, clearly separated by NMDS1 axis. ECM fungi also affected bacterial community structures in mesh bags. The result of CCA analysis showed the effects of ECM fungi on the bacterial community structure in mesh bags (Fig. 5b). Detailed analyses revealed that the top 10 ECM fungi observed in mesh bags explained 65.75% of the total variance in bacterial community structure, suggesting that these fungi do have an impact on bacterial community. In addition, mantel test was used to assess the correlation between ECM genera and bacterial community, which further indicated that *Trichophaea* and *Tuber* were significantly related to changes in the bacterial community ($r = 0.39$, $p < 0.01$; $r = 0.37$, $p < 0.01$).

The functional traits in the mesh bags were predicted using PICRUSt, showing that member transport, signal transduction, cell mobility and environmental adaption were more active in mineral-filled mesh bags compared to the control bags (Fig. S2). However, carbohydrate metabolism was the most active metabolic pathway in the control, accounting for 14.26 ± 0.06%.

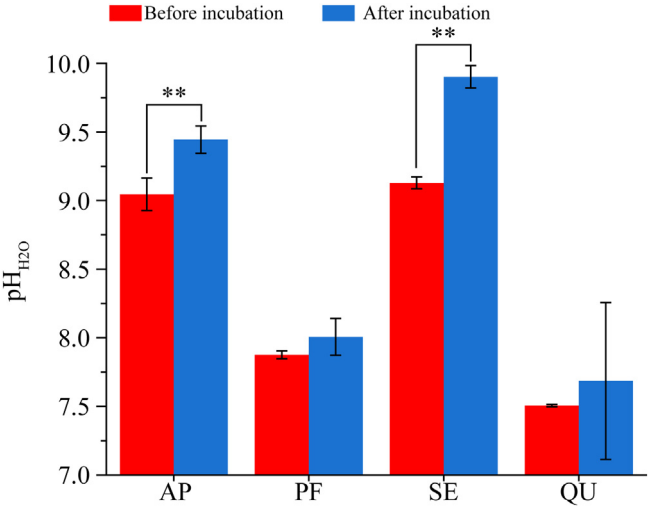

Fig. 1. pH values in different mineral-filled mesh bags (b). AP: apatite-filled mesh bags, PF: potash feldspar-filled mesh bags, QU: quartz-filled mesh bags (the control), SE: serpentine-filled mesh bags. Asterisks above error bars signify significant differences between before and after incubation identified by *t*-test. $^{**}p < 0.01$.

4. Discussion

After six months of incubation in situ, the content of available elements and pH_{H2O} in the mesh bags were significantly different. All

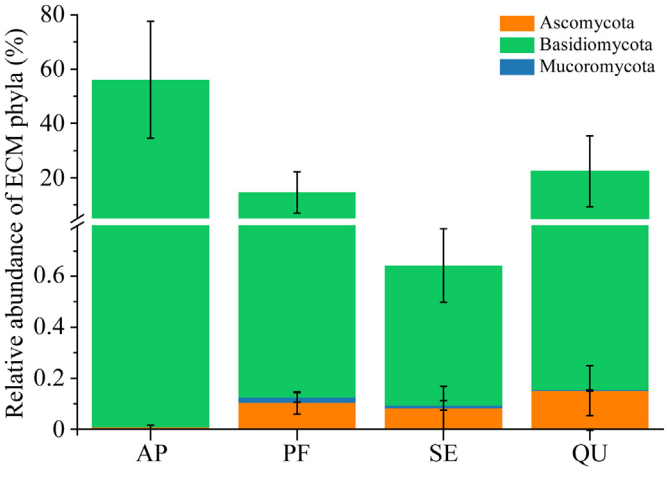

Fig. 2. Proportion of ECM phyla in different mesh bags.

Table 2
α-Diversity indices of different treatments.

Treatment	OTU	Chao1	Simpson	Shannon
AP	3306 ± 467^{ab}	4112 ± 432^{a}	0.01 ± 0.00^{bc}	6.40 ± 0.35^{b}
PF	3048 ± 150^{b}	3870 ± 157^{a}	0.02 ± 0.01^{ab}	5.77 ± 0.25^{c}
SE	2574 ± 162^{c}	3226 ± 323^{b}	0.03 ± 0.01^{a}	5.10 ± 0.25^{d}
QU	3822 ± 119^{a}	4292 ± 162^{a}	0.00 ± 0.00^{c}	7.03 ± 0.10^{a}

Different letters indicate significant differences among different treatments based on Tukey's HSD tests at $p < 0.05$.

mesh bags were colonized by diverse bacteria and ECM fungi. The fungi in the apatite-filled bags were mainly of ECM origin, similar to the results found by Bastias et al. (2006) and Hedh et al. (2008). However, the proportion of ECM fungi in the serpentine-filled bags was extremely low, even lower than that in the control bags. This indicated that mineral substrate has an impact on the colonization of ECM fungi. The average amount of ECM genera and ECM OTUs detected in the apatite-filled bags was the lowest among the mesh bags (Table S1), which suggested that only a few ECM species can obtain P in apatite. *Trichophaea* and *Sebacina* were the dominant ECM genera in the apatite-filled bags, suggesting they may be pioneers in apatite weathering. In this study, these two genera were not only detected in the apatite-filled bags but also detected in other bags, which suggested that ECM fungi may have a priority in colonizing mineral based on their mineral-weathering abilities. The ECM genera of *Cortinarius*, *Meliniomyces*, *Rhizopogon* and *Russula* documented with the ability to weather apatite (i.e. Nygren and Rosling, 2009; Rosling et al., 2004; Wallander et al., 2002) were also identified in the apatite-filled bags. Ectomycorrhizal fungi were dominant fungal taxa in the apatite-filled bags (Fig. 2), which may be because P was deficient (0.21 mg P/kg soil) in the area of this study. The study of (Bai et al., 2020) suggested that ECM fungal communities are more abundant in the nutrient-poor environments than in the nutrient-rich environments. In this situation, apatite in the mesh bags is the main source of P that can be directly acquired by ECM fungi. In the potash feldspar-filled bags, ECM species were the most abundant, including 56 OTUs, which indicated that more ECM species are capable of weathering potash feldspar. Compared to the apatite-filled bags, the ratio of ECM sequences to total fungal sequences in the potash feldspar-filled bags was much lower, which may be closely related to the available content of K in the forest soil, which was low but not deficient. The proportion of ECM fungi was extremely low in serpentine-filled bags. This may be due to the content of available Mg (122.68 mg/kg soil) was not limited to plants and ECM fungi in this forest. Ectomycorrhizal fungi can obtain Mg through direct absorption from bulk soil by extensive underground fungal network without the need to weather mineral through extensively colonizing the serpentine-filled bags. These results suggested that ECM fungi may adopt different strategies, such as by weathering soil minerals or direct mycelial absorption (Landeweert et al., 2001; Cairney, 2011), to obtain mineral nutrients based on the availability of nutrients in forest soils. In addition, OTU1 (*Trichophaea* sp.), OTU3 (*Sebacina* sp.), OTU56 (*Chloridium* sp.), OTU440 (*Lactarius crassiusculus*) OTU784 (*Cortinarius* sp.), OTU1269 (*Piloderma bicolor*), OTU2123 (*Ceratobasidium* sp.), were identified in different treatments (Table S1), suggesting that these fungi have the potential to acquire nutrients from different minerals. *Trichophaea* was the most dominant ECM genus in all mesh bags, suggesting this genus of fungi possess high weathering potential and may play an essential role in acquiring nutrients from soil minerals/rocks in forests.

Bacterial community structure and composition in different mesh bags was markedly distinct (Fig. 5a). Uroz et al. (2012) proposed the concept of mineralosphere and suggested that the characteristics of mineral are a key driving force affecting bacterial community. The bacterial community structure in mineralosphere in the soil is not only affected by mineral types (Gleeson et al., 2006; Carson et al., 2009; Ahmed and Holmström, 2015), but also is affected by other edaphic factors such as soil pH, humidity, oxygen and root exudates, etc. (Chan et al., 2012). However, effects of ECM fungi on bacterial community structure are rarely taken into account. In this study, it showed significant relationship between ECM fungi and bacterial community structure in mesh bags (Fig. 5b), which may benefit to the weathering of minerals. Our results showed the number of bacterial OTUs in mineral-filled mesh bags was lower than that in the control (Table 2), echoing the results of Uroz et al. (2010) that ECM fungi do not increase the genetic diversity of bacterial communities in the soil. It showed that the bacterial diversity in mineral-filled bags was lower than that in the control bags (Table 2), but showed much higher population sizes in apatite-, potash feldspar- and serpentine-filled bags (Fig. 6). The bacterial communities in different mineral-filled bags had remarkable differences (Figs. 3, 4), suggesting that bacterial diversity is affected by ECM fungi and soil minerals.

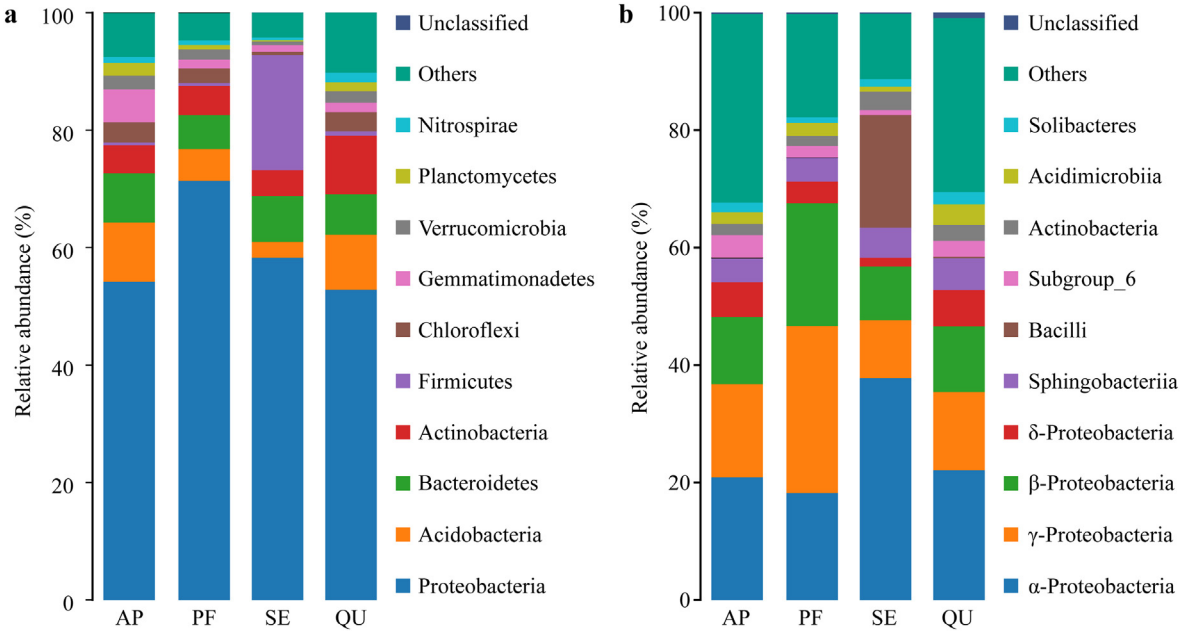

Fig. 3. Bacterial composition at (a) phylum and (b) class levels in different mesh bags.

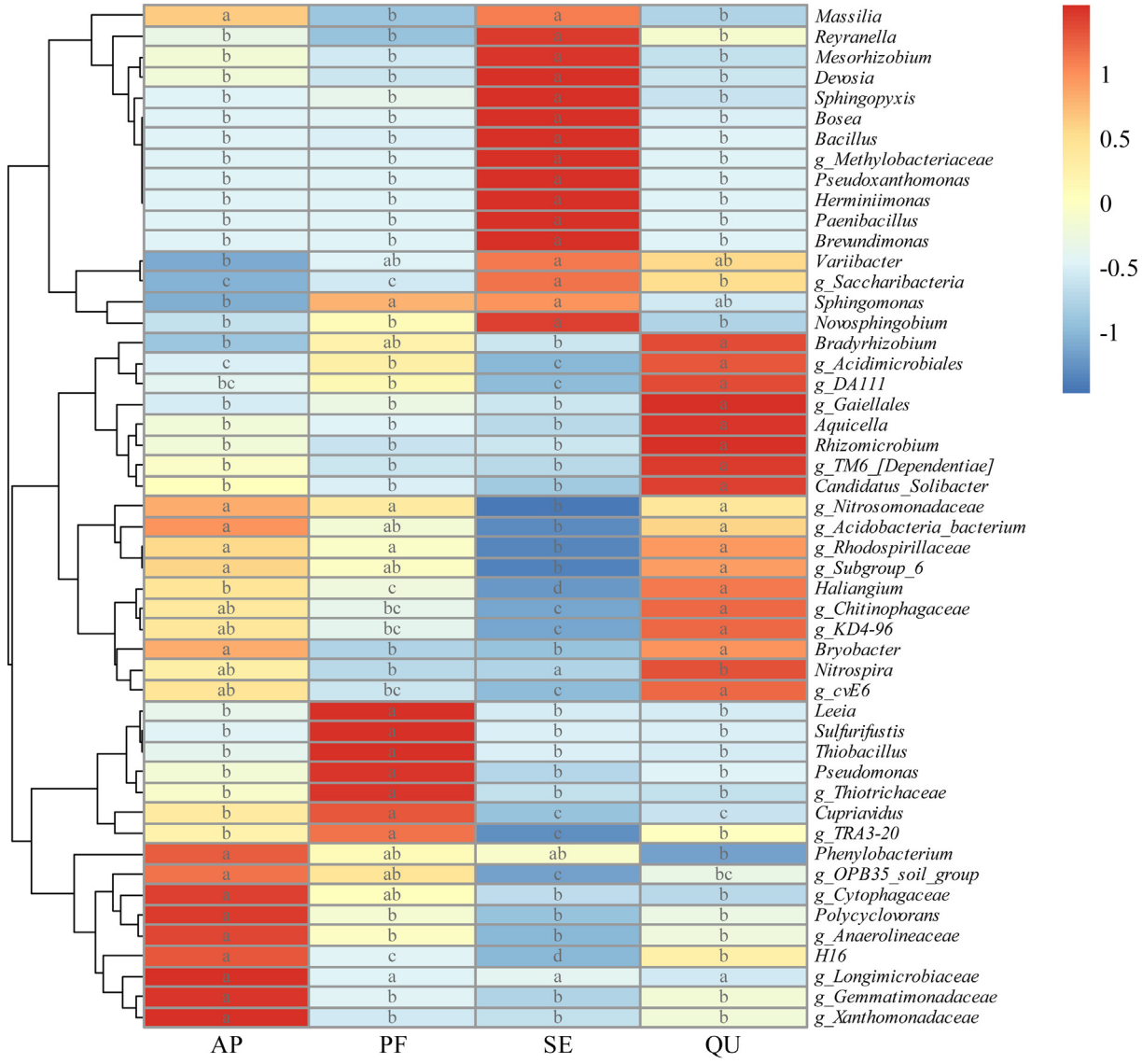

Fig. 4. Heatmap of bacterial composition of the top 50 genera. The same letter in each rectangular box in the same row denotes no significant difference identified by Tukey's HSD tests at $p < 0.05$.

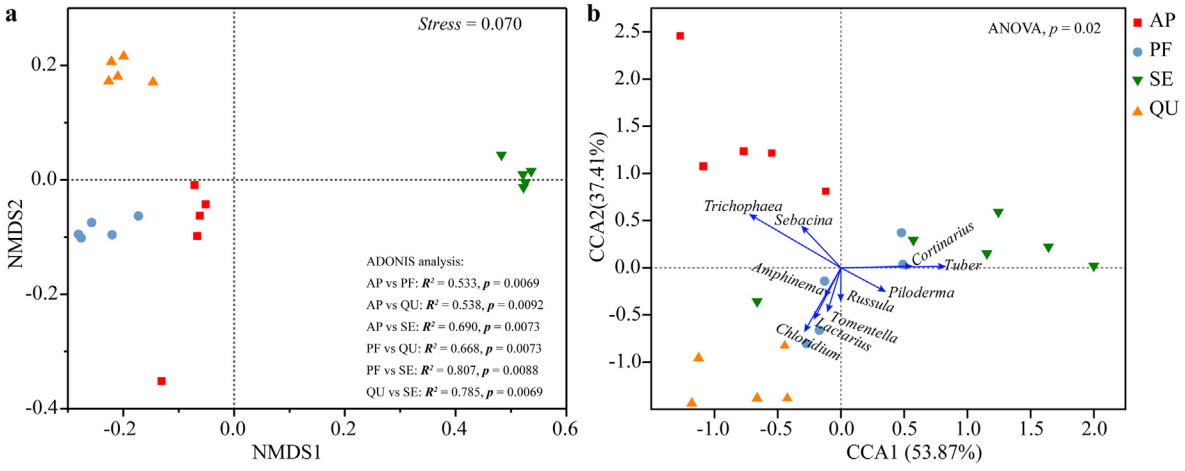

Fig. 5. (a) Two-dimensional NMDS plots of bacterial communities based on Bray-Curtis dissimilarity and (b) the impact of the most abundance 10 ECM genera on bacterial community structures in different mesh bags.

Ectomycorrhizal fungi in soils are able to locally enrich associated bacterial numbers (Olsson and Wallander, 1998; Heinonsalo et al., 2001), such as to enrich bacteria with high mineral-weathering potential thus to promote mineral dissolution (Frey-Klett et al., 2005; Calvaruso et al., 2010). Proteobacteria *Pseudomonas* and *Sphingomonas*, well-known with high mineral-weathering potential (Uroz et al., 2007; Nicolitch et al., 2016; Colin et al., 2017), were the dominant genera in apatite- and potash feldspar-filled bags. However, Firmicutes *Bacillus* and *Paenibacillus* with high mineral-weathering potential (Sheng et al., 2008; Liu et al., 2012) had the highest relative abundance in serpentine-filled bags. This suggested that ECM fungi are able to affect mineral-weathering bacteria to promote mineral weathering based on mineral types. It is well known that ECM fungi can secret secondary metabolites to recruit special bacteria (Johansson et al., 2004; Duponnois and Kisa, 2006; Bonfante and Anca, 2009), indicating signal communication occurs between the fungi and bacteria. The results of predicted functional traits showed that signal transduction and cell mobility were significantly more active in apatite-, potash feldspar- and serpentine-filled bags than those in the control bags (Fig. S2), which indicated that bacteria respond to signals from ECM fungi and move toward them. The neutral dispersal of bacteria in soils is extremely slow, limited by soil water content and the expression of flagella or other mobility factors supporting bacterial movement (Dechesne et al., 2010). Therefore, special attraction mechanisms by ECM fungi may be responsible for the formation of mineral-weathering bacterial communities. Some studies documented that bacteria are able to move and disperse on 'fungal highways', and colonize in environments where they alone would be difficult to colonize (Simon et al., 2017; Whitman et al., 2018). Vik et al. (2013) also proposed that the specific bacterial communities in ectomycorrhizae may be transported from the surrounding soil using ECM fungal hyphae as a transport vector. The underground ECM fungal hyphae may be an important factor to affect bacterial communities. Additionally, the process of carbohydrate metabolism was much more active in the control bags, presumed due to the lack of carbon source. The bacteria in the control bags were lack of simple and easy-to-use carbon sources and had to decompose a variety of complex organic substances infiltrated from outside to meet their needs for carbon sources and energy. This also explained why the relative abundance of actinomycetes in the control bags was higher compared to other mesh bags (Fig. 3a), because actinomycetes in soils are considered as major decomposers of complex organic matter such as lignocellulosic polymers and can utilize complex mechanisms to utilize them (Sonia et al., 2011).

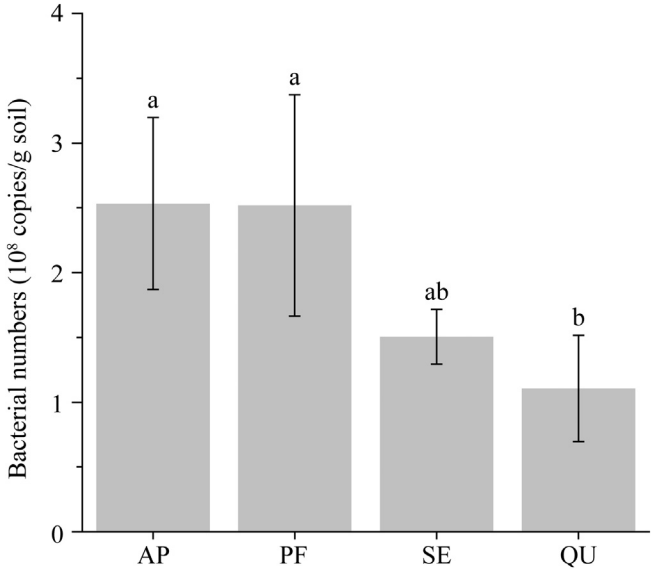

Fig. 6. Bacterial population sizes in different mesh bags.

5. Conclusions

This study demonstrated that impacts of mineral types on the composition of ECM fungi and bacteria using in-growth mesh bags in situ. The fungi were mostly ECM in apatite-filled bags and the lowest proportion of ECM fungi in serpentine-filled bags, showing these fungi have a preference for minerals in colonization, and the genus *Trichophaea* is the dominant ECM species. Ectomycorrhizal fungi and minerals may have impacts on bacterial community structure and metabolisms cooperatively. This study reveals relationships of ECM fungi and soil bacteria under the impact of mineral substrate, enhancing the understanding of the role of fungi-bacteria interactions in soil mineral weathering and plant nutrition.

Supplementary data to this article can be found online at https://doi.org/10.1016/j.scitotenv.2020.137663.

CRediT authorship contribution statement

Qibiao Sun: Investigation, Formal analysis, Writing - original draft. **Xiuming Liu:** Resources, Writing - review & editing, Funding acquisition. **Shijie Wang:** Writing - review & editing, Supervision. **Bin Lian:** Conceptualization, Writing - review & editing, Supervision, Funding acquisition.

Declaration of competing interest

The authors declare that they have no conflict of interest.

Acknowledgements

The authors extend their gratitude to the two anonymous reviewers for their insightful comments and kindly suggestions. We also thank Dr. Shameer Syed (College of Life Sciences, Nanjing Normal University) for English polishing and constructive comments on this manuscript. This work was supported by Strategic Priority Research Program of the Chinese Academy of Sciences (grant number XDA23060102) and the National Natural Science Foundation of China (grant number 41772360).

References

Ahmed, E., Holmström, S.J.M., 2015. Microbe–mineral interactions: the impact of surface attachment on mineral weathering and element selectivity by microorganisms. Chem. Geol. 403, 13–23.
Averill, C., Hawkes, C.V., 2016. Ectomycorrhizal fungi slow soil carbon cycling. Ecol. Lett. 19, 937–947.
Bai, Z., Yuan, Z.-Q., Wang, D.-M., Fang, S., Ye, J., Wang, X.-G., Yuan, H.-S., 2020. Ectomycorrhizal fungus-associated determinants jointly reflect ecological processes in a temperature broad-leaved mixed forest. Sci. Total Environ. 703, 135475.
Bastias, B.A., Xu, Z., Cairney, J.W., 2006. Influence of long-term repeated prescribed burning on mycelial communities of ectomycorrhizal fungi. New Phytol. 172, 149–158.
Blum, J.D., Klaue, A., Nezat, C.A., Driscoll, C.T., Johnson, C.E., Siccama, T.G., Eagar, C., Fahey, T.J., Likens, G.E., 2002. Mycorrhizal weathering of apatite as an important calcium source in base-poor forest ecosystems. Nature 417, 729–731.
Bonfante, P., Anca, I.A., 2009. Plants, mycorrhizal fungi, and bacteria: a network of interactions. Annu. Rev. Microbiol. 63, 363–383.
Bonneville, S., Smits, M.M., Brown, A., Harrington, J., Leake, J.R., Brydson, R., Benning, L.G., 2009. Plant-driven fungal weathering: early stages of mineral alteration at the nanometer scale. Geology 37, 615–618.
Bonneville, S., Bray, A.W., Benning, L.G., 2016. Structural Fe(II) oxidation in biotite by an ectomycorrhizal fungi drives mechanical forcing. Environ. Sci. Technol. 50, 5589–5596.
Cairney, J.W.G., 2011. Ectomycorrhizal fungi: the symbiotic route to the root for phosphorus in forest soils. Plant Soil 344, 51–71.
Calvaruso, C., Turpault, M.-P., Leclerc, E., Ranger, J., Garbaye, J., Uroz, S., Frey-Klett, P., 2010. Influence of forest trees on the distribution of mineral weathering-associated bacterial communities of the *Scleroderma citrinum* mycorrhizosphere. Appl. Environ. Microbiol. 76, 4780–4787.
Carson, J.K., Campbell, L., Rooney, D., Clipson, N., Gleeson, D.B., 2009. Minerals in soil select distinct bacterial communities in their microhabitats. FEMS Microbiol. Ecol. 67, 381–388.
Chan, Y., Lacap, D.C., Lau, M.C.Y., Kong, Y.H., Warren-Rhodes, K.A., Cockell, C.S., Cowan, D.A., Mckay, C.P., Pointing, S.B., 2012. Hypolithic microbial communities: between a rock and a hard place. Environ. Microbiol. 14, 2272–2282.

Colin, Y., Nicolitch, O., Turpault, M.P., Uroz, S., 2017. Mineral types and ree species determine the functional and taxonomic structures of forest soil bacterial communities. Appl. Environ. Microbiol. 83, e02684-16.
Dechesne, A., Wang, G., Gulez, G., Or, D., Smets, B.F., 2010. Hydration-controlled bacterial motility and dispersal on surfaces. Proc. Natl. Acad. Sci. 107, 14369–14372.
Duponnois, R., Kisa, M., 2006. The possible role of trehalose in the mycorrhiza helper bacterium effect. Can. J. Bot. 84, 1005–1008.
Edgar, R.C., 2013. UPARSE: highly accurate OTU sequences from microbial amplicon reads. Nat. Methods 10, 996–998.
Edgar, R.C., Haas, B.J., Clemente, J.C., Quince, C., Knight, R., 2011. UCHIME improves sensitivity and speed of chimera detection. Bioinformatics 27, 2194–2200.
Ekblad, A., Mikusinska, A., Agren, G.I., Menichetti, L., Wallander, H., Vilgalys, R., Bahr, A., Eriksson, U., 2016. Production and turnover of ectomycorrhizal extramatrical mycelial biomass and necromass under elevated CO_2 and nitrogen fertilization. New Phytol. 211, 874–885.
Frey-Klett, P., Chavatte, M., Clausse, M.L., Courrier, S., Le Roux, C., Raaijmakers, J., Martinotti, M.G., Pierrat, J.C., Garbaye, J., 2005. Ectomycorrhizal symbiosis affects functional diversity of rhizosphere fluorescent pseudomonads. New Phytol. 165, 317–328.
Gardes, M., Bruns, T.D., 1993. ITS primers with enhanced specificity for basidiomycetes - application to the identification of mycorrhizae and rusts. Mol. Ecol. 2, 113–118.
Genney, D.R., Anderson, I.C., Alexander, I.J., 2006. Fine-scale distribution of pine ectomycorrhizas and their extramatrical mycelium. New Phytol. 170, 381–390.
Gleeson, D., Mcdermott, F., Clipson, N., 2006. Structural diversity of bacterial communities in a heavy metal mineralized granite outcrop. Environ. Microbiol. 8, 383–393.
Hagenbo, A., Clemmensen, K.E., Finlay, R.D., Kyaschenko, J., Lindahl, B.D., Fransson, P., Ekblad, A., 2017. Changes in turnover rather than production regulate biomass of ectomycorrhizal fungal mycelium across a *Pinus sylvestris* chronosequence. New Phytol. 214, 424–431.
Hedh, J., Wallander, H., Erland, S., 2008. Ectomycorrhizal mycelial species composition in apatite amended and non-amended mesh bags buried in a phosphorus-poor spruce forest. Mycol. Res. 112, 681–688.
Heinemeyer, A., Hartley, I.P., Evans, S.P., Carreira, De La Fuente, J.A., Ineson, P., 2007. Forest soil CO_2 flux: uncovering the contribution and environmental responses of ectomycorrhizas. Glob. Chang. Biol. 13, 1786–1797.
Heinonsalo, J., Jørgensen, K.S., Sen, R., 2001. Microcosm-based analyses of Scots pine seedling growth, ectomycorrhizal fungal community structure and bacterial carbon utilization profiles in boreal forest humus and underlying illuvial mineral horizons. FEMS Microbiol. Ecol. 36, 73–84.
Johansson, J.F., Paul, L.R., Finlay, R.D., 2004. Microbial interactions in the mycorrhizosphere and their significance for sustainable agriculture. FEMS Microbiol. Ecol. 48, 1–13.
Koele, N., Dickie, I.A., Blum, J.D., Gleason, J.D., de Graaf, L., 2014. Ecological significance of mineral weathering in ectomycorrhizal and arbuscular mycorrhizal ecosystems from a field-based comparison. Soil Biol. Biochem. 69, 63–70.
Kõljalg, U., Nilsson, R.H., Abarenkov, K., Tedersoo, L., Taylor, A.F., Bahram, M., Bates, S.T., Bruns, T.D., Bengtsson-Palme, J., Callaghan, T.M., 2013. Towards a unified paradigm for sequence-based identification of fungi. Mol. Ecol. 22, 5271–5277.
Landeweert, R., Hoffland, E., Finlay, R.D., Kuyper, T.W., van Breemen, N., 2001. Linking plants to rocks: ectomycorrhizal fungi mobilize nutrients from minerals. Trends Ecol. Evol. 16, 248–254.
Langille, M.G.I., Zaneveld, J., Caporaso, J.G., McDonald, D., Knights, D., Reyes, J.A., Clemente, J.C., Burkepile, D.E., Vega Thurber, R.L., Knight, R., Beiko, R.G., Huttenhower, C., 2013. Predictive functional profiling of microbial communities using 16S rRNA marker gene sequences. Nat. Biotechnol. 31, 814.
Lapeyrie, F., Ranger, J., Vairelles, D., 1991. Phosphate-solubilizing activity of ectomycorrhizal fungi *in vitro*. Can. J. Bot. 69, 342–346.
Lindahl, B.D., Ihrmark, K., Boberg, J., Trumbore, S.E., Högberg, P., Stenlid, J., Finlay, R.D., 2007. Spatial separation of litter decomposition and mycorrhizal nitrogen uptake in a boreal forest. New Phytol. 173, 611–620.
Liu, D., Lian, B., Dong, H., 2012. Isolation of *Paenibacillus* sp. and assessment of its potential for enhancing mineral weathering. Geomicrobiol J. 29, 413–421.
Magoč, T., Salzberg, S.L., 2011. FLASH: fast length adjustment of short reads to improve genome assemblies. Bioinformatics 27, 2957–2963.
Nicolitch, O., Colin, Y., Turpault, M.P., Uroz, S., 2016. Soil type determines the distribution of nutrient mobilizing bacterial communities in the rhizosphere of beech trees. Soil Biol. Biochem. 103, 429–445.
Nygren, C.M.R., Rosling, A., 2009. Localisation of phosphomonoesterase activity in ectomycorrhizal fungi grown on different phosphorus sources. Mycorrhiza 19, 197–204.
Olsson, P.A., Wallander, H., 1998. Interactions between ectomycorrhizal fungi and the bacterial community in soils amended with various primary minerals. FEMS Microbiol. Ecol. 27, 195–205.
Paris, F., Botton, B., Lapeyrie, F., 1996. *In vitro* weathering of phlogopite by ectomycorrhizal fungi. Plant Soil 179, 141–150.
Parks, D.H., Tyson, G.W., Hugenholtz, P., Beiko, R.G., 2014. STAMP: statistical analysis of taxonomic and functional profiles. Bioinformatics 30, 3123.
R Core Team, 2016. R: A Language and Environment for Statistical Computing. R Foundation for Statistical Computing, Vienna, Austria URL. https://www.R-project.org/.
Rosling, A., Lindahl, B.D., Taylor, A.F., Finlay, R.D., 2004. Mycelial growth and substrate acidification of ectomycorrhizal fungi in response to different minerals. FEMS Microbiol. Ecol. 47, 31–37.
Schloss, P.D., Westcott, S.L., Ryabin, T., Hall, J.R., Hartmann, M., Hollister, E.B., Lesniewski, R.A., Oakley, B.B., Parks, D.H., Robinson, C.J., Sahl, J.W., Stres, B., Thallinger, G.G., van Horn, D.J., Weber, C.F., 2009. Introducing mothur: open-source, platform-independent, community-supported software for describing and comparing microbial communities. Appl. Environ. Microbiol. 75, 7537–7541.
Sheng, X.F., Zhao, F., Yan, H.L., Qiu, G., Chen, L., 2008. Isolation and characterization of silicate mineral-solubilizing *Bacillus globisporus* Q12 from the surfaces of weathered feldspar. Can. J. Microbiol. 54, 1064–1068.
Simon, A., Herve, V., Al-Dourobi, A., Verrecchia, E., Junier, P., 2017. An *in situ* inventory of fungi and their associated migrating bacteria in forest soils using fungal highway columns. FEMS Microbiol. Ecol. 93, fiw217.
Smith, S.E., Read, D., 2008. Mycorrhizal Symbiosis. Elsevier Academic Press Inc, Netherlands.
Smits, M.M., Bonneville, S., Benning, L.G., Banwart, S.A., Leake, J.R., 2012. Plant-driven weathering of apatite–the role of an ectomycorrhizal fungus. Geobiology 10, 445–456.
Soltanpour, P.N., 1985. Use of ammonium bicarbonate DTPA soil test to evaluate elemental availability and toxicity. Commun. Soil Sci. Plant Anal. 16, 323–338.
Sonia, M.-T., Naceur, J., Abdennaceur, H., 2011. Studies on the ecology of actinomycetes in an agricultural soil amended with organic residues: I. Identification of the dominant groups of Actinomycetales. World J. Microbiol. Biotechnol. 27, 2239–2249.
Sun, Q., Lian, B., 2019. The different roles of *Aspergillus nidulans* carbonic anhydrases in wollastonite weathering accompanied by carbonation. Geochim. Cosmochim. Acta 244, 437–450.
Sun, Q., Fu, Z., Finlay, R.D., Lian, B., 2019. Transcriptome analysis provides novel insights into the capacity of the ectomycorrhizal fungus *Amanita pantherina* to weather K-containing feldspar and apatite. Appl. Environ. Microbiol. 85, e00719-19.
Tedersoo, L., Hansen, K., Perry, B.A., Kjøller, R., 2006. Molecular and morphological diversity of pezizalean ectomycorrhiza. New Phytol. 170, 581–596.
Tedersoo, L., May, T.W., Smith, M.E., 2010. Ectomycorrhizal lifestyle in fungi: global diversity, distribution, and evolution of phylogenetic lineages. Mycorrhiza 20, 217–263.
Uroz, S., Calvaruso, C., Turpault, M.P., Pierrat, J.C., Mustin, C., Frey-Klett, P., 2007. Effect of the mycorrhizosphere on the genotypic and metabolic diversity of the bacterial communities involved in mineral weathering in a forest soil. Appl. Environ. Microbiol. 73, 3019–3027.
Uroz, S., Calvaruso, C., Turpault, M.P., Frey-Klett, P., 2009. Mineral weathering by bacteria: ecology, actors and mechanisms. Trends Microbiol. 17, 378–387.
Uroz, S., Buee, M., Murat, C., Frey-Klett, P., Martin, F., 2010. Pyrosequencing reveals a contrasted bacterial diversity between oak rhizosphere and surrounding soil. Environ. Microbiol. Rep. 2, 281–288.
Uroz, S., Turpault, M.P., Delaruelle, C., Mareschal, L., Pierrat, J.-C., Frey-Klett, P., 2012. Minerals affect the specific diversity of forest soil bacterial communities. Geomicrobiol. J. 29, 88–98.
van Schöll, L., Smits, M.M., Hoffland, E., 2006. Ectomycorrhizal weathering of the soil minerals muscovite and hornblende. New Phytol. 171, 805–814.
Vik, U., Logares, R., Blaalid, R., Halvorsen, R., Carlsen, T., Bakke, I., Kolstø, A.-B., Økstad, O.A., Kauserud, H., 2013. Different bacterial communities in ectomycorrhizae and surrounding soil. Sci. Rep. 3, 3471.
Wallander, H., 2000. Uptake of P from apatite by *Pinus sylvestris* seedlings colonised by different ectomycorrhizal fungi. Plant Soil 218, 249–256.
Wallander, H., Nilsson, L.O., Hagerberg, D., Bååth, E., 2001. Estimation of the biomass and seasonal growth of external mycelium of ECM fungi in the field. New Phytol. 151, 753–760.
Wallander, H., Johansson, L., Pallon, J., 2002. PIXE analysis to estimate the elemental composition of ectomycorrhizal rhizomorphs grown in contact with different minerals in forest soil. FEMS Microbiol. Ecol. 39, 147–156.
Wang, W., Sun, Q., Lian, B., 2018. Redox of fungal multicopper oxidase: a potential driving factor for the silicate mineral weathering. Geomicrobiol. J. 35, 879–886.
White, T.J., Bruns, T., Lee, S., Taylor, J., 1990. Amplification and direct sequencing of fungal ribosomal RNA genes for phylogenetics. In: Michael, A.I., David, H.G., John, J.S., Thomas, J.W. (Eds.), PCR Protocols: A Guide to Methods and Applications. Academic Press, pp. 315–322.
Whitman, T., Neurath, R., Perera, A., Chu-Jacoby, I., Ning, D., Zhou, J., Nico, P., Pett-Ridge, J., Firestone, M., 2018. Microbial community assembly differs across minerals in a rhizosphere microcosm. Environ. Microbiol. 20, 4444–4460.